

Neutrinos and gamma-rays of hadronic origin from AGN jets

A. M. Atoyan,^a C. D. Dermer^b

^a*CRM, Universite de Montreal, Montreal H3C 3J7, Canada*

^b*E. O. Hulburt Center for Space Research, Code 7653, Naval Research Laboratory, Washington, DC 20375-5352*

Abstract

We discuss the fluxes of high energy neutrinos and gamma-rays expected from AGNs if hadrons can be effectively accelerated to ultra-high energies by their relativistic jets, as currently believed. Fluxes of multi-TeV neutrinos detectable by *km*-scale detectors like *IceCube* could be expected from powerful blazars where strong accretion-disk radiation is present in the AGN cores. Gamma-ray fluxes of hadronic origin can be important for flares in the compact jets of these sources up to GeV energies, but they will be insignificant for BL Lac objects. Production of UHE neutral beams composed of neutrons and gamma-rays can drive straight collimated jets in the intergalactic medium on multi-kpc scales, which could be resolved by the Chandra X-ray observatory. While we do not expect any significant neutrino flux from these large-scale jets, we predict gamma-rays of synchrotron origin in the energy range from sub-GeV up to TeV energies, which would be detectable by GLAST and ground-based gamma-ray telescopes.

Key words: galaxies: active — gamma-rays: theory — jets — neutrinos

1 Introduction

AGN jets, along with GRBs, are powerful accelerators of relativistic particles, and the prime candidate sources of extra-galactic cosmic rays (CRs) with energy spectra extending beyond 10^{20} eV. Detections of non-thermal flares from blazars in the X-ray and particularly in the γ -ray domain in the last decade have convincingly demonstrated that the compact inner (*sub-parsec scale*) jets of blazars do accelerate particles to very high energies (1; 2), presumably due to relativistic shocks. Although analyses of correlated X-ray and TeV gamma-ray flares in BL Lacs support leptonic models (3; 4; 5; 6), which imply efficient acceleration of relativistic electrons, the associated acceleration of hadrons is

expected with at least the same efficiency as that of the leptons. It might be different in electron-positron pair jets where few hadrons would be present, but comparison of the radio lobe and inner jet powers indicates that jets are composed mainly of electrons and protons (7), so that a nonthermal hadronic component is very plausible.

Observational evidence for acceleration of hadrons in the jets of AGN requires a target for interactions in the jets. In principle, ultrarelativistic protons accelerated in the inner jets up to energies $\sim 10^{20}$ eV could produce synchrotron emission detectable at TeV energies (8; 9), but this requires extremely strong magnetic fields ~ 20 -100 G in the sub-parsec scale jets. All other observable consequences of hadron acceleration result from interactions with ambient material or photon fields. These include neutrinos, detection of which would provide a direct proof for hadron acceleration, and the high energy electromagnetic radiation from the secondary leptons and γ -rays. Such evidence could also be provided by production of collimated beams of ultra-high energy (UHE; $\gg 10^{15}$ eV for the discussion below) neutrons and gamma-rays formed in the same process of hadronic interactions, which could explain effective transport of energy from AGN cores to multi-kpc scales (10).

2 Neutrinos and gamma-rays from compact jets

Interaction cross sections of relativistic protons and nuclei with targets in astrophysical environments are generally not as large as cross sections of relativistic electrons. Therefore one would expect that observable radiation of hadronic origin might be produced first of all in compact relativistic jets at sub-parsec scales where the target, be it gas or photons, still remains sufficiently dense. One group of hadronic jet models invokes nuclear interactions with ambient matter (11; 12) through the process $p + p \rightarrow \pi^{\pm,0} \rightarrow \nu, e^{\pm}, \gamma$. Nuclear interaction models require, however, large masses, resulting in uncomfortably large total energy in the jet (10), which includes kinetic energy of the blob and the energy of relativistic protons needed for production of the observed γ -ray fluxes.

A second group of hadronic models is based upon photomeson interactions of relativistic hadrons with ambient photon fields in the jet. The relevant proton-photon processes are $p + \gamma \rightarrow p + \pi^0$ followed by $\pi^0 \rightarrow 2\gamma$, and $p + \gamma \rightarrow n + \pi^+$, followed by $\pi^{\pm} \rightarrow \mu^{\pm} + \nu_{\mu} \rightarrow e^{\pm} + 2\nu_{\mu} + \nu_e$. The same pool of secondaries is produced in multi-pion production channels, and it is important to notice that in about half of all these inelastic collisions the primary relativistic proton will be converted to a relativistic neutron.

Most of the photohadronic models take into account collisions of high-energy

protons with the internal synchrotron photons (13; 14; 15), while others also take into account external radiation that originates either directly from the accretion disk (16) or from disk radiation that is scattered by surrounding clouds to form a quasi-isotropic radiation field (17). BL Lac objects have weak emission lines, so in these sources the dominant soft photon field is thought to be the internal synchrotron emission. The strong optical emission lines from the illumination of BLR clouds in FSRQs reveal luminous accretion-disk and scattered disk radiation.

The photomeson interaction threshold is about 150 MeV in the rest frame of the proton, which requires ultra-high energies for the accelerated particles to be above threshold for optical/UV photons. In the case of internal synchrotron radiation, the energy output of secondary particles formed in photohadronic processes is generally peaked in the energy range from $\approx 10^{16}$ - 10^{18} eV in either low- or high-frequency peaked BL Lac objects (15), which implies that such models can only be efficient if protons are accelerated to even higher energies. This demand upon proton acceleration for efficient photomeson production on the *internal* synchrotron photons also holds for FSRQs, which have similar nonthermal soft radiation spectra as low-frequency peaked BL Lac objects. However the presence of the isotropic external radiation field of UV/soft X-ray energies in the central ~ 0.1 -1 parsec broad-line emission region (BLR) of FSRQs both substantially increases the photomeson production efficiency and relaxes the requirement of very high proton energies needed for $p\gamma$ interactions (17). Another important feature of the external radiation target is that, unlike the internal radiation, it does not dilute in the course of rapid expansion of the jet/blob, and is available for photomeson interactions during all the time of propagation of UHE protons through the BLR.

In the model of Atoyan and Dermer (17; 10), protons are accelerated in an outflowing plasma blob moving with bulk Lorentz factor Γ along the symmetry axis of the accretion-disk/jet system. These protons are assumed to have an isotropic pitch-angle distribution in the comoving frame of a plasma blob, within which is entrained a tangled magnetic field. Using the parameters of the non-thermal flares detected from the FSRQ blazar 3C279 and from the BL Lac object Mkn 501 as prototypes, the fluxes of high-energy neutrinos and gamma-rays (of hadronic origin) are calculated (10) assuming that the power to accelerate relativistic protons is equal to the power injected into relativistic electrons needed to explain the non-thermal flares detected by EGRET (18) and BeppoSax (5).

Fig. 1a (*left panel*) shows the spectra of neutrons escaping the blob (heavy solid curve) and then the BLR (dashed curve) for 3C279, calculated for the variability time $t_{var} = 1$ d and the jet's Doppler-factor $\delta = 10$, which defines the blob size $R \leq t_{var}c\delta/(1+z)$. The dot-dashed curve shows the spectrum of the gamma-rays produced by the neutrons outside the blob (but within

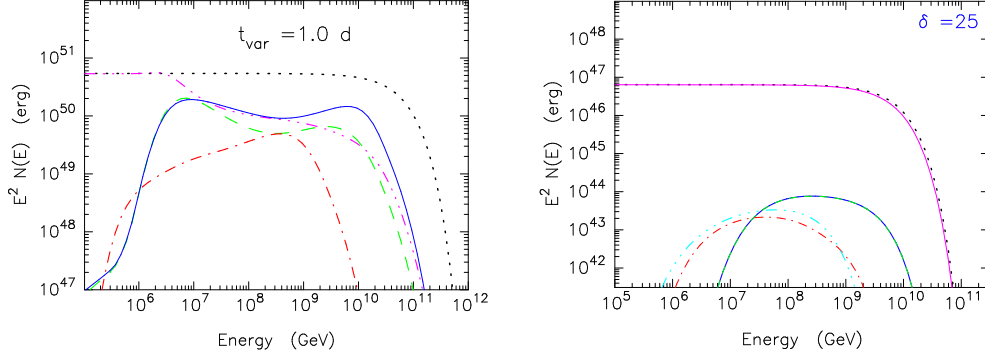


Fig. 1. **a** (left panel): Spectra of protons injected into the blob (dotted curve), protons which remain in the blob when it reaches the edge of the BLR (thin solid curve), neutrons escaping from the blob (thick solid curve), and escaping neutrons (dashed curve) and gamma rays (dot-dashed curves) which reach the edge of the BLR, calculated for 3C279 flare parameters assuming $\delta = 10$; **b** (right panel): Similar particle spectra as on the left panel, but calculated for the parameters of the flare of Mkn 501, assuming $t_{var} = 0.3$ d and $\delta = 25$. In addition, here we also show by 3-dot-dashed curve the spectra of neutrinos produced in the blob.

the BLR), and which therefore can escape the absorption on the internal synchrotron photons inside the blob. The dotted curves show the overall spectra of protons injected into the blob, assuming that injection has occurred during the time $\simeq t_{var}$, and the thin solid curves show the spectra of protons which remain in the blob by the time that the blob reaches the edge of the BLR. The fraction of the total energy of injected protons which is taken away by the UHE neutrons with $E_n \geq 10^{17}$ eV and the γ -rays with $E_\gamma \geq 10^{16}$ eV is generally at the level of $\sim 10\%$ of the total energy injected in UHE protons. These numbers become dramatically lower, dropping down by orders of magnitude, in the case of BL Lac-type objects where the external radiation field is almost absent, so that the intensity of photomeson interactions relies only upon the internal synchrotron field. This is demonstrated in Fig. 1b using flare parameters of Mkn 501. Note that the UHE gamma-ray fluxes shown in Fig. 1b by dashed-dotted curve are produced predominantly *inside* the blob, but because of much lower density of the internal radiation these gamma-rays may have a chance (depending also on δ) to avoid $\gamma\gamma$ pair-production absorption.

Fig. 2 shows the integrated neutrino fluences over the time it takes for the blob to pass through the BLR in 3C 279. The solid and dashed curves show the fluence calculated for $\delta = 6$ and 10, respectively. The thick and thin curves represent the fluence of neutrinos produced in photomeson interactions inside and outside the blob, respectively. For the spectral fluence shown in Fig. 2, the total number of neutrinos that could be detected by a km^3 detector such as *IceCube*, using calculated neutrino detection efficiencies (19), are 0.37 for $\delta = 6$, and 0.21 for $\delta = 10$. These numbers could be several times larger if the jet power that goes to acceleration of protons is higher than that of the electrons, implying hadronically dominated jets. We note, however, that the

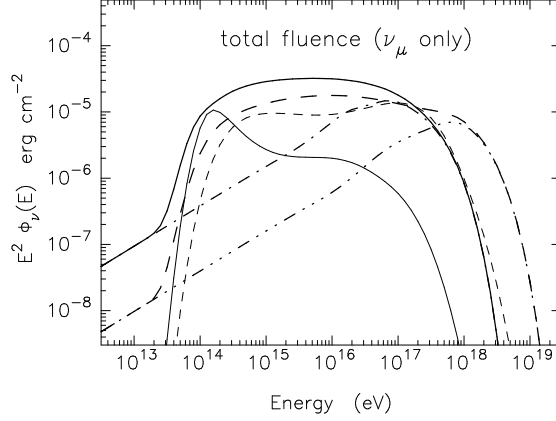


Fig. 2. Fluences of neutrinos integrated over several days in the observer frame determined by the time for the blob to pass through the BLR in 3C279. The solid and dashed curves show the fluences calculated for $\delta = 6$ and 10, and the thick and thin curves represent the fluences of neutrinos produced by photopion interactions inside and outside the blob, respectively. The dot-dashed and 3-dot – dashed curves show the fluences due to $p\gamma$ collisions if external radiation field is not taken into account.

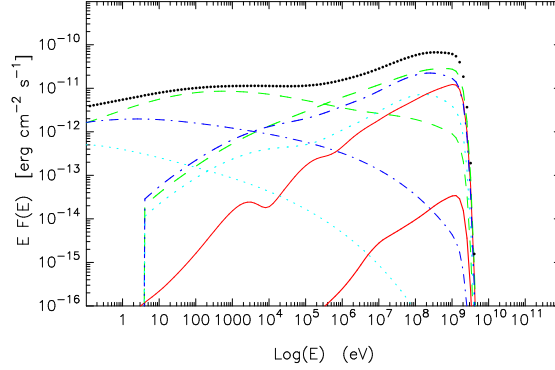


Fig. 3. Radiation flux produced in and escaping from the blob (full dots) following the electromagnetic cascade initiated by energetic electrons and gamma rays produced in photopion interactions, calculated for the parameters of 3C 279 flare in case of $\delta = 10$. The thick and thin curves correspond to synchrotron and Compton radiations, respectively. The radiation of the first generation of electrons, which includes the electrons produced by absorption of π^0 -decay γ -rays in the blob, is shown by the solid curves. The dashed, dot-dashed and 3-dot-dashed curves show contributions from the 2nd, 3rd and 4th generations of cascade electrons, respectively.

neutrinos can be expected not only during the flares, but also in periods between the active flares, insofar as the EGRET observations show a persistent *average* level of gamma-ray fluxes from 3C 279 at the level of $\sim 10\%$ of the flare flux, implying persistent electron/proton acceleration. Since the external photon target is always available, over the course of one year several neutrinos should be detected from FSRQs such as 3C 279 with km-scale neutrino detectors. The presence of a quasi-isotropic external radiation field becomes crucial for neutrino detection, which results in the prediction that FSRQs will be

detected with km-scale neutrino detectors, whereas BL Lac objects are much less promising for neutrino detection (17; 10).

We also calculated (10) the associated radiation from the cascades induced by photohadronic processes in the compact jets. Fig. 3 shows the multiple generations of cascade radiation and the total emergent flux associated with the neutrino production given in Fig. 2. Purely hadronic models could be effective for interpretation of gamma-ray fluxes only up to GeV energies observed from FSRQs by EGRET. At higher energies, the hadronic fluxes would be absorbed in the external UV radiation field if it is sufficiently dense to be effective for photomeson interactions. If the source is transparent to TeV radiation, as in case of BL Lac objects, the intensity of photohadronic processes would be consequently low. Fig. 2 also shows that the efficiency of proton acceleration is limited by the intensity of the cascade radiation. In particular, X-ray observations of 3C 279 limit the ratio of proton-to-electron acceleration powers in the flaring state to a factor ≤ 10 .

3 Radiation from the large-scale jets

Because the UHE neutrons and gamma-rays are produced quasi-isotropically in the comoving frame of a relativistically moving source with $\Gamma_{jet} \sim 10$, for the external observer they are collimated in a beam with a characteristic opening angle $\theta \sim 1/\Gamma \sim$ few degrees. As our calculations show (10), the energy contained in this neutral beam in case of FSRQs can reach a few percent of the total energy injected in accelerated hadrons in the compact sub-parsec jet, which is very substantial. Thus, for the jets in 3C 279 this would correspond to a mean power for UHE neutral beam production $\sim 10^{45}$ erg/s. This power is then transported to large distances from the compact nucleus, and is released in the processes of neutron decay (17; 10), $n \rightarrow p + e + \nu$, and $\gamma\gamma \rightarrow e^\pm$ attenuation (20; 17) on the cosmic microwave background radiation field. The neutron decay paths are $l_{n.d.} \simeq 1 (E/10^{17} \text{ eV}) \text{ kpc}$, i.e. in the range $\sim 1 \text{ kpc} - 1 \text{ Mpc}$ for $E_n \sim 10^{17}-10^{20} \text{ eV}$. This is similar to the $\gamma\gamma$ -interaction pathlengths for the gamma-rays with energies $10^{16}-10^{19} \text{ eV}$. These decay distances agree with the length scales of the straight narrow jets resolved by the Chandra X-ray observatory from a number of AGN. Therefore neutral beams may provide a new interpretation for the origin of these jets, given that there is a mechanism for the conversion of the energy and momentum of the charged particles emerging from the neutral beam into the surrounding intergalactic medium, with subsequent electron acceleration out of the thermal pool. The latter is required for the interpretation of the synchrotron fluxes of these jets detected at radio and optical wavelengths.

For the UHE gamma-ray component of the neutral beam, we note that the

emerging $e^+ - e^-$ pairs would almost immediately lose their energy by synchrotron radiation in the ambient magnetic fields with a transverse (to the jet direction) component $B_\perp \sim 1 \mu\text{G}$ or larger. The cooling path of these electrons, l_{cool} , is typically much shorter than their gyroradius:

$$l_{cool}/R_{gyr} \simeq 0.2(B_\perp 1 \mu\text{G})^{-1} (E_e/10^{17} \text{ eV})^{-2},$$

which implies that these electrons would not exert any significant pressure on the ambient medium. The energy of these electrons will be converted into γ -rays with characteristic energies $\epsilon_{syn} \simeq 4 (B_\perp/10 \mu\text{G}) (E_e/10^{17} \text{ eV})^2 \text{ GeV}$.

For the beam of parent gamma-rays with E_γ from $\sim 10^{16}$ to $> 10^{18} \text{ eV}$, the synchrotron γ -ray fluxes in the characteristic jet magnetic fields $\sim 10 \mu\text{G}$ should appear at sub-GeV to TeV energies. These synchrotron gamma-rays would be strongly polarized, the detection of which could support their hadronic origin. Another, albeit less conclusive, feature of the synchrotron gamma-ray fluxes would consist in the detection of atypically hard spectral indices, with most of the energy flux peaked at high energies due to the sharp cutoff in the production spectra of $e^+ - e^-$ pairs below 10^{16} eV . These fluxes could be detectable by GLAST at GeV energies, and at higher energies by the ground-based gamma-ray telescopes with energy thresholds well below 100 GeV, like HESS, VERITAS, etc. The sensitivity of these instruments is at the energy flux level $f_{-12} \equiv f_\epsilon \sim 10^{-12} \text{ erg cm}^{-2} \text{ s}^{-2} \sim 1$ or better (2; 21). This implies an apparent “ 4π ” luminosity of the source at a distance $d = d_{Gpc} \text{ Gpc}$ at the level of $L_{4\pi} \simeq 10^{44} f_{-12} d_{Gpc}^2 \text{ erg/s}$. For comparison, the *absolute* power of the neutral beam for the parameters used for 3C279 is at the level $L_{beam} \sim 10^{45} \text{ erg/s}$.

The energy and momentum of the neutron component of the beam after the β -decay goes primarily to the protons. There is no effective target for interactions of these protons with the intergalactic medium, except via the magnetic field. Any significant deflection of the protons from their initial direction implies that a beam of β -decay protons should transfer its momentum to the surrounding medium to drive turbulence which could effectively deposit both the beam energy and momentum along its path. Driving the intergalactic medium into motion will cause stretching of the ambient magnetic field, whatever its initial orientation, along the beam, as is observed in large-scale jets. Thus, the UHE neutrons of the neutral beam represent the main component for driving and continuously supplying power into the large scale jets. Electrons from the ambient medium accelerated in the first or second order Fermi process could explain the synchrotron fluxes extending up to the X-ray domain (22). Interestingly, the $e^+ e^-$ pairs from the gamma-ray beam, or even the β -decay electrons of the neutron beam, might lead to a two-component synchrotron models which seem to be needed for consistent interpretation of optical/X-ray data in some jets like Pictor A.

It is important to note that this method of energy transport up to Mpc scales

by neutral UHE beam avoids quenching of the jet by material both in dense central region on parsec scales, and in the intergalactic medium on multi-kpc scales. Acceleration of hadrons in the compact jets of AGN also implies that most of the UHE protons would accumulate in time in the central region of AGN at the parsec scales after deceleration of the inner jet. A partial degradation of the energy of these protons with $E_p \sim 10^{15} - 10^{16}$ eV in the photomeson collision with the accretion disk radiation would initiate Mpc-scale halos (23) around such FSRQs, due to pair cascades on the CMBR, which might be detectable by forthcoming gamma-ray telescopes.

Acknowledgments. AA appreciates the financial support provided by the LOC. The work of CD is supported by the Office of Naval Research and NASA grant DPR S-13756G.

References

- [1] Hartman, R. C., et al., *ApJS* **123** (1999) 79
- [2] Weekes, T. C., in *High Energy Gamma-Ray Astronomy*, F. A. Aharonian and H. J. Völk, eds., AIP: New York (2001) 15
- [3] Mastichiadis, A. & Kirk, J. G. *Astron. Astrophys.* **320** (1997) 19
- [4] Catanese, M. et al. *Astrophys. J.* **487** (1997) L143
- [5] Pian, E. et al. *Astrophys. J.* **492** (1998) L17
- [6] Krawczynski, H., Coppi, P. S., & Aharonian, F., *MNRAS* **336** (2002) 721
- [7] Celotti, A. & Fabian, A. C., *M.N.R.A.S.* **264** (1993) 228
- [8] Aharonian, F. A. *New Astronomy* **5** (2000) 377
- [9] Mücke, A. & Protheroe, R. J. *Astroparticle Physics* **15** (2001) 121
- [10] Atoyan, A. M., & Dermer, C. D., *Astrophys. J.* **586** (2003) 79
- [11] Beall, J. H. & Bednarek, W. *Astrophys. J.* **510** (1999) 188
- [12] Schuster, C., Pohl, M., & Schlickeiser, R. *Astron. Astrophys.* **382**(2002) 829
- [13] Mannheim, K., and Biermann, P.L. *Astron. Astrophys.* **253** (1992) L21
- [14] Mannheim, K., *Astron. Astrophys.* **269** (1993) 67
- [15] Mücke, A., et al., *Astropart. Phys.* **18** (2002) 593
- [16] Bednarek, W., and Protheroe, R. J. *MNRAS* **302** (1999) 373
- [17] Atoyan, A., & Dermer, C. D., *Phys. Rev. Letters* **87** (2001) 221102
- [18] Wehrle, A. E. et al., *Astrophys. J.* **497** (1998) 178
- [19] Gaisser, T. K., Halzen, F., & Stanev, T., *Phys. Reports* **258** (1995) 173
- [20] Neronov, A., et al. *Phys. Rev. Letters* **89** (2002) 51101
- [21] Aharonian, F. A., et al. *Astropart. Phys.* **6** (1997) 343
- [22] Dermer, C. D., and Atoyan, A. *Astrophys. J.* **568** (2002) L81
- [23] Aharonian, F. A., Coppi, P. S., & Völk, H. J. *Astrophys. J.* **423** (1994) L5